Journal of Marine Systems 79 (2010) 245–257

Contents lists available at ScienceDirect

Journal of Marine Systems

journal homepage: www.elsevier.com/locate/jmarsys

Climate change, teleconnection patterns, and regional processes forcing marine populations in the Pacific

Franklin B. Schwing [a,*], Roy Mendelssohn [a], Steven J. Bograd [a], James E. Overland [b], Muyin Wang [b], Shin-ichi Ito [c]

[a] Environmental Research Division, Southwest Fisheries Science Center, NOAA Fisheries Service, 1352 Lighthouse Avenue, Pacific Grove, CA 93950-2097, United States
[b] Pacific Marine Environmental Laboratory, National Ocean and Atmosphere Administration, Seattle, Washington, United States
[c] Tohoku National Fisheries Research Institute, Fisheries Research Agency 3-27-5, Shinhama-cho, Shiogama-city, Miyagi 985-0001, Japan

ARTICLE INFO

Article history:
Received 11 April 2007
Received in revised form 6 April 2008
Accepted 24 November 2008
Available online 20 February 2009

Keywords:
Climate change
Teleconnections
Marine ecosystems
Pacific Ocean

ABSTRACT

Climate change impacts in large marine ecosystems (LMEs) are driven by global climate variability, often communicated over large distances by atmospheric teleconnections, and modified by the dominant local and regional ocean processes. The focus of this paper is to summarize the key processes and features that characterize the major coastal LMEs of the Pacific, as part of a greater effort to understand the role of past and future global climate change in driving (possibly synchronous) fluctuations in marine populations. The physical setting of five LMEs – the Humboldt Current System (HCS), California Current System (CCS), Gulf of Alaska (GOA), Kuroshio Current System (KCS), and Oyashio Current System (OCS) – and the mechanisms and impacts of climate variability on these systems are described. Because of their pivotal role in linking and perhaps synchronizing climate variability in disparate LMEs, we also review teleconnections and analyze past global atmospheric teleconnections and regional ocean response patterns. The major Pacific eastern boundary current systems, the CCS and HCS, feature similar dominant processes (e.g., coastal upwelling), and share atmospheric forcing from common teleconnection patterns that vary together. Sea level pressure variations forcing the KCS and OCS systems on climate scales, however, are not strongly teleconnected to the CCS and HCS. A common factor analysis of sea surface temperature (SST) within these ecosystems provides an example of how LMEs have responded to past climate variability. All LMEs display a persistent warming tendency since 1900, with multi-decadal fluctuations superimposed. However, SST fluctuations in the western Pacific lag those in the east by about a decade. Global synchrony in climate forcing is modulated by distinct processes within each LME, which reduce the correlation between long-term fluctuations.

Published by Elsevier B.V.

1. Introduction

Marine ecosystems are sensitive to perturbations in their physical environment on all time scales, particularly those comparable to the lifespan of their longer-lived top predator species. Climate events, notably interannual events such as ENSO, and variations on decadal and longer scales, appear to force often-dramatic shifts in the production, distribution, and biomass of many marine populations as well as the overall productivity and organization of their ecosystems. Thus, if disparate populations and biologically unconnected ecosystems change simultaneously (Alheit and Bakun, 2010, and citations therein), they are most likely responding to ocean basin-scale or global climate variability.

There are difficulties with moving beyond correlational physical–biological relationships to ascribing the mechanisms responsible for ecosystem variability. Long-term tendencies can be hidden in the seasonal and non-seasonal components of climate time series (Mendelssohn et al., 2003, 2004). Ecosystems may have a long memory of past climate events (Percival et al., 2001); for example, the impacts of El Niño events may be seen in marine systems for several years. Even identifying when variations are significant from noise or random fluctuations is a complex problem (Pierce et al., 2000; Pierce, 2001; Newman et al., 2003; Overland et al., 2006).

It is critical to understand how physical climate signals propagate, and what processes lead to ecosystem change. Climate variations are communicated through fluxes of heat, moisture, and momentum by atmospheric circulation, and via the transport of heat, buoyancy, momentum, and material by the large-scale ocean circulation. The former appear to occur in recognizable patterns of variability via teleconnections (Horel and Wallace, 1981; Wallace and Gutzler, 1981). These propagations lead to regional signals that alter the processes that determine ecosystem form, function, and productivity. They often are summarized by spatial patterns and temporal indices that characterize the time variability of climate, and are commonly used as climate indices.

* Corresponding author. Tel.: +1 831 648 9034; fax: +1 831 648 8440.
E-mail address: Franklin.Schwing@noaa.gov (F.B. Schwing).

0924-7963/$ – see front matter. Published by Elsevier B.V.
doi:10.1016/j.jmarsys.2008.11.027

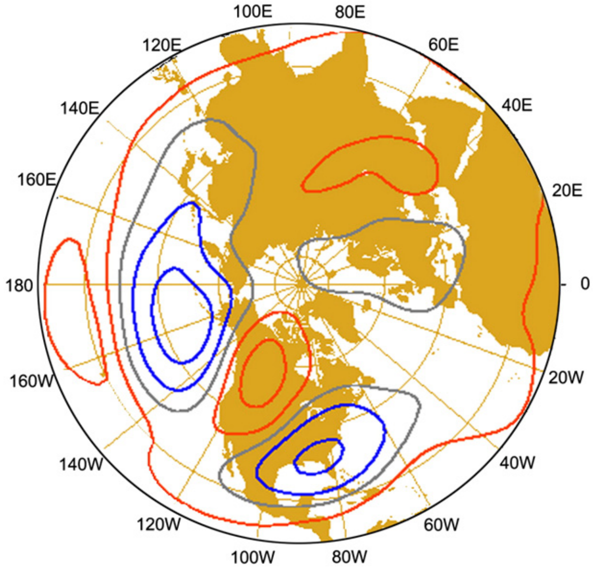

Fig. 1. Schematic of the mean atmospheric pressure pattern in the northern hemisphere. The distribution of high (red contours) and low (blue contours) pressure centers highlights the Pacific–North American teleconnection pattern. The positive phase of the PNA is associated with positive anomalies over the North Pacific and western North America, and negative anomalies over the Gulf of Alaska and the southeastern US.

Since teleconnections are important in forcing and transmitting climate signals globally, the focus here is to describe their impact, the potential mechanisms that force ecosystem change, and the interactions of global climate forcings with regional processes and features within individual ecosystems (and at sub-ecosystem scales) that modulate them.

In this paper, we summarize the key processes and features that characterize the major coastal large marine ecosystems (LMEs) of the Pacific Ocean – the Humboldt Current System (HCS), California Current System (CCS), Gulf of Alaska (GOA), Kuroshio Current System (KCS), and Oyashio Current System (OCS) – with emphasis on those processes important to marine fishery populations. To set the stage, an overview of atmospheric teleconnections is provided, and evidence is given for teleconnections (and the lack thereof) between various ocean regions. Second, we characterize the impact of past climate variability on these features, identifying the mechanisms linking global climate to regional ocean responses and future climate change scenarios. Third, we compare the response of the LMEs with respect to the similarities in the processes, the timing of their fluctuations, and probable teleconnections. Our goal is to describe the basics of signals of climate forcing in these LMEs from past variability, which will assist fisheries scientists in understanding climate-ecosystem linkages and determine the probable consequences of future climate change to marine ecosystems and their primary fishery populations.

2. Teleconnections

Atmospheric teleconnections (Gu and Philander, 1997; Alexander et al., 2004) transmit climate signals over very long distances to remote ecosystems, where local environmental conditions and physiography modify their impacts on the biology. Teleconnections are a way of summarizing atmospheric patterns and interactions, as well as describing the transport processes for heat, moisture, and momentum — the 'fuels' of the Earth's climate. They are important to understand as vectors of climate variability that drive conditions affecting land and ocean. They also provide a way of integrating and quantifying climate variability into a small set of indices. Finally, recognizing teleconnection patterns as they occur and evolve allows better understanding of regional climate change, assessments at the ecosystem scale and the likely consequences to marine populations.

It has long been recognized that global atmospheric pressure systems are linked on interannual and longer time scales (Walker, 1924). Atmospheric teleconnections link widely separated pressure centers (Namias, 1959, 1969; Horel and Wallace, 1981; Barnston and Livezey, 1987), allowing redistributions in atmospheric mass associated with El Niño/La Niña, decadal, and other climate scales to create well-defined anomaly patterns. This has allowed climate scientists to identify pressure-based indices that characterize and quantify climate variability. The teleconnection indices of most importance to the LMEs of concern here include the Southern Oscillation (SO, Walker, 1924), the Pacific/North American Index (PNA, Wallace and Gutzler, 1981), the North Atlantic Oscillation (NAO, Barnston and Livezey, 1987), the Arctic Oscillation (AO, also called the Northern Annular Mode; Thompson and Wallace, 1998; Overland and Wang, 2005), and the North Pacific Index (NPI, Trenberth and Hurrell, 1994). The PNA, for example, characterizes a pattern that connects the Pacific and Atlantic regions (Fig. 1).

Fig. 2 displays schematically the atmospheric teleconnection between the equatorial Pacific and the mid-latitude high-pressure systems that control wind forcing in the Pacific's eastern boundary current (EBC) ecosystems. Low pressure in the western tropical Pacific results in a tropospheric signal that feeds the extra-tropical North and South Pacific Highs (NPH and SPH), which drive coastal upwelling and much of the ocean circulation and structure in the CCS and HCS, respectively. Air rises in tropical convective systems (shown schematically as clouds) and then flows poleward and eastward as upper tropospheric winds. It then descends over the mid-latitude regions of the eastern Pacific. Trade winds in the lower troposphere return from the NPH and SPH into an area of low sea level pressure (SLP) in the western tropical Pacific–southeast Asian region.

This circuit, called the Hadley–Walker circulation (Peixoto and Oort, 1992), has a mean symmetry about the equator that extends over the North and South Pacific basins. Through this circulation, the NPH and SPH contribute to climate variations of Southeast Asia and the

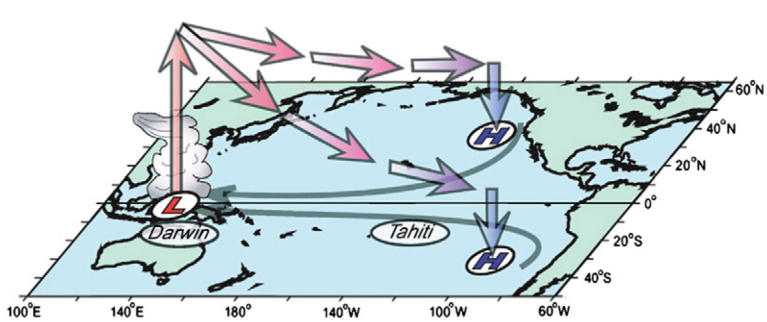

Fig. 2. Schematic of the mean Hadley–Walker atmospheric (teleconnections) circulation in the Pacific region. Predominant pressure systems, Darwin Low and North and South Pacific Highs, denoted by L and H symbols, respectively. Smaller arrows denote near-surface trade winds; larger arrows reflect upper troposphere winds.

tropical Indo-Pacific region. On intraseasonal to interannual scales, SLP variations at the NPH and SPH tend to be out of phase with the western tropical Pacific. A perturbation anywhere within this circulation will impact the entire system (Schwing et al., 2002). For example, an El Niño event weakens the equatorial low in the western Pacific, which will weaken the extra-tropical highs and the trades that connect them. In general, therefore, anomalies in these high-pressure systems will be similar on interannual time scales, so anomalies in the forcing of the CCS and HCS are likely to coincide as well. However, this is not always the case, and the asymmetry of the seasons and differences in latitude of these systems complicates the issue. Since this is a coupled system, extra-tropical perturbations (e.g., modifications of the NPH or SPH by perturbations in the jet stream) may trigger equatorial variability as well.

Teleconnections can also propagate over long distances through the ocean, via planetary and coastal-trapped waves. The most familiar of these are the internal Kelvin waves generated by perturbations of the pycnocline in the equatorial Pacific as the ocean component of ENSO (cf. Philander, 1990; Delcroix et al., 1991). These propagate east along the equator, and are frequently, but not always, seen as poleward propagations along the west coast of North and South America (Enfield and Allen, 1980; Pares-Sierra and O'Brien, 1989; Clarke and Lebedev, 1999) They can transfer their signals across the equatorial Pacific in a matter of weeks, and to the mid-latitudes in another few months. As these Kelvin waves propagate along the eastern boundaries, their energy is scattered into slower-moving Rossby waves that propagate west. These have been observed to move across the North Pacific on ca. 10 years (Jacobs et al., 1994), a possible source of decadal variability in the ocean basins. Coastal Kelvin waves also can be generated by factors such as regional meteorological forcing (e.g., frontal passages, tropical storms), so their signals may be confused with those generated in the tropics. Because the HCS is closer to the equator, Kelvin waves are more significant off South America. Rossby waves are also generated by regional atmospheric-forced disturbances and can appear as anomalies in regional ocean circulation and vertical structure on interannual scales (Lynn et al., 1995).

Interannual and decadal variability in atmospheric circulation on upper ocean conditions have been the subject of several studies (Namias, 1959, 1969; Trenberth and Hurrell, 1994; Tomita et al., 2001). Schwing et al. (2002) identified a “characteristic spatial relationship” between anomalies in atmospheric pressure and upper ocean temperature in the North Pacific, suggesting that atmospheric and oceanic variability are coupled on intraseasonal, interannual, and interdecadal scales. Tomita et al. (2002) recognized the importance of atmospheric and ocean dynamics to interdecadal variations in North Pacific sea surface temperature (SST). Ocean anomalies are communicated to other basins via atmospheric teleconnections, also referred to as the ‘atmospheric bridge’ (Lau, 1997; Alexander et al., 2002). Through this atmospheric bridge, SST anomalies in the Pacific contribute to variations in SST in the Atlantic and Indian Oceans (Klein et al., 1999; Mo and Hakkinen, 2001; White and Allan, 2001).

An Empirical Orthogonal Function (EOF)/Principal Component Analysis (PCA) is one way of objectively characterizing the primary spatial patterns of variance. From a PCA of Northern Hemisphere winter atmospheric pressure, Quadrelli and Wallace (2004) concluded that just two spatial patterns explain much of the variability in familiar teleconnection patterns (Fig. 3). The first pattern is, by

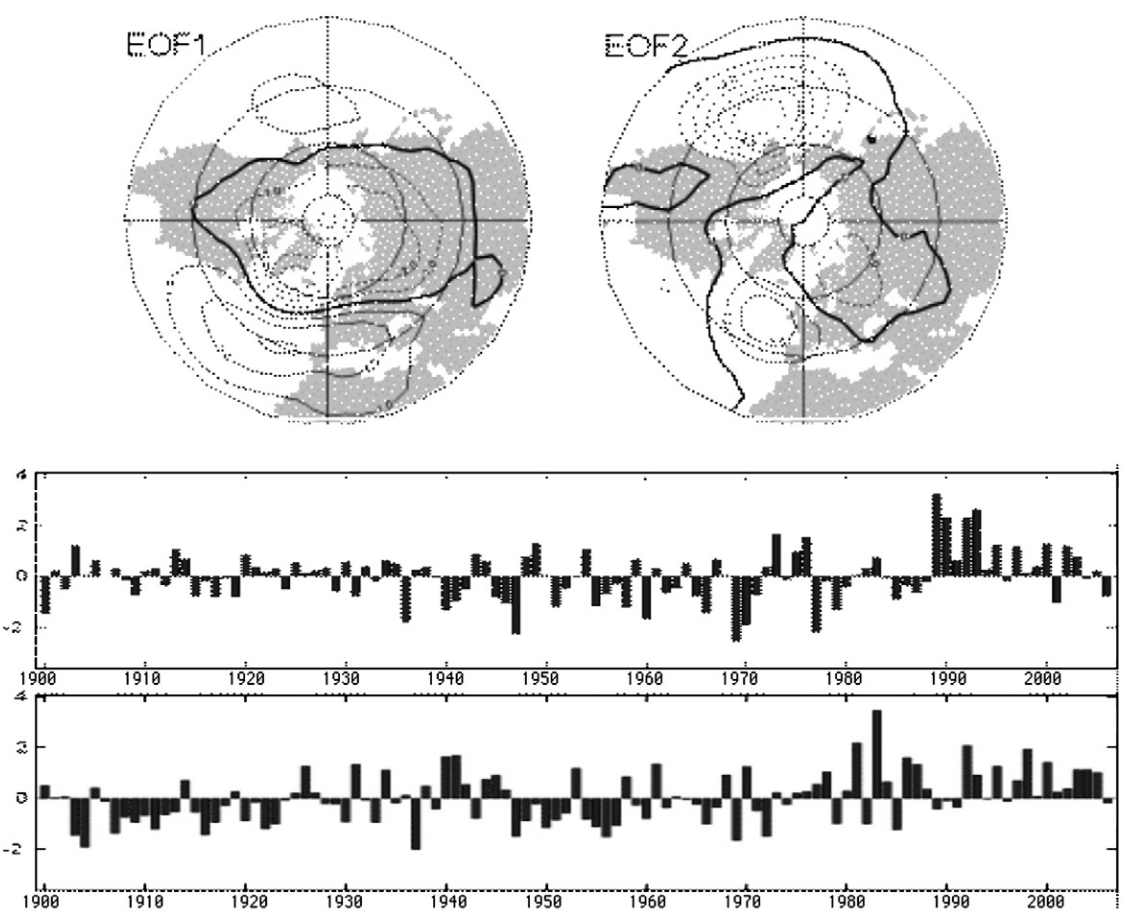

Fig. 3. Leading two modes of the EOFs for northern hemisphere winter (DJFM) SLP (1900–2006). The spatial pattern of the first mode is similar to the AO, and explains 22.6% of the total variance. Time series is positive when Arctic SLP is low. The second mode reflects the PNA pattern and explains 12.3% of total variance. Time series is positive when North Pacific SLP is low. After Quadrelli and Wallace (2004).

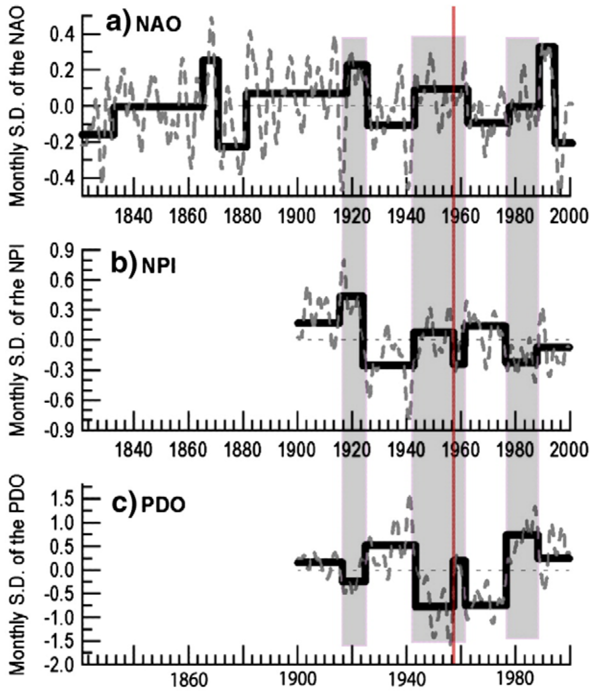

Fig. 4. Time series of (a) NAO (1821–2000), (b) NPI (1899–2000), and (c) PDO (1899–2000) indices (dashed lines). Series smoothed with a 39-month Gaussian filter. Bold lines show significant climate regimes and change points ("regime shifts") determined from objective analysis for abrupt changes (from Schwing et al., 2003).

definition, the AO. The second pattern resembles the PNA in the Pacific (cf. Fig. 1). Positive signs to the two PCA time series indicate lower and higher SLP over the Atlantic and Pacific, respectively, and correlate with warmer temperatures over the land masses to their east. Beyond these first two modes, most atmospheric variability is less systematic. These two patterns, which explain about one-third of the total SLP variance, also incorporate the variability described by a number of familiar atmospheric indices, including the NAO, NPI, and the Pacific Decadal Oscillation (PDO). The times series show the strong AO event in the early 1990s and a weak but positive PNA-like Pacific pattern since 1976, negative values through the 1950s and a long upward trend for the first 30 years of the 20th century. In addition to these patterns, interannual components of the SLP field appear to be part of a global structure symmetrical about the equator, with a strong tropical influence from ENSO.

2.1. Global teleconnections: linking climate variability between the Pacific and Atlantic

One of the intriguing challenges is identifying if marine ecosystems world-wide are fluctuating in synchrony, as suggested by the long time series of a number of fish populations (Lluch-Belda et al., 1992; Hare and Mantua, 2000; McFarlane et al., 2000). In particular, do populations co-vary in Pacific and Atlantic ecosystems? If so, does coherent forcing drive biological variability, and are disparate marine populations responding to the same climate signal? Teleconnections, as described above, are a likely mechanism for communicating climate variability between these ocean basins.

The AO and PNA are two teleconnection patterns that link the Atlantic and Pacific regions (Figs. 1, 3). These atmospheric modes imply stable, predictable spatial patterns of climate variability. However, these spatial patterns change over time. A number of studies suggest that climate variations in the Atlantic and Pacific are not coupled. Tomita et al. (2001) characterized decadal-scale variability in global atmospheric circulation and SST as having independent patterns associated with the SO, NAO, and NPI. Trenberth and Hurrell (1994) showed that winter atmospheric SLP over the North Pacific, which is dominated by interannual and interdecadal variability, has a strong negative correlation with a SST spatial pattern later identified by Mantua et al. (1997) as the PDO. However, North Pacific and North Atlantic SLP variations are poorly correlated (Trenberth and Hurrell, 1994; Hurrell,1996). Similar studies (Thompson and Wallace, 1998; Tomita et al., 2001) found a negative correlation between the PDO and NPI, but only weak correlations between North Pacific SLP and the NAO.

Abrupt changes in atmospheric and ocean circulation on interdecadal time scales (regime shifts) are linked between the Atlantic and Pacific (Schwing et al., 2003), but not always with the same phase sign (Fig. 4). Indices for both basins show simultaneous shifts at about 1915, 1924, 1942, 1961, 1976, and 1988. The longer NAO also displays regime shifts at these times, as well as in 1832, 1865, 1870, and 1881. Shifts in the NAO and NPI (PDO) were positively (negatively) correlated prior to the late 1950s. However this relationship breaks down after about 1961, suggesting that although the North Atlantic and North Pacific atmosphere is teleconnected on multidecadal scales, it has multiple spatial modes. These results imply there are periods when the Atlantic and Pacific ecosystems are forced in the same

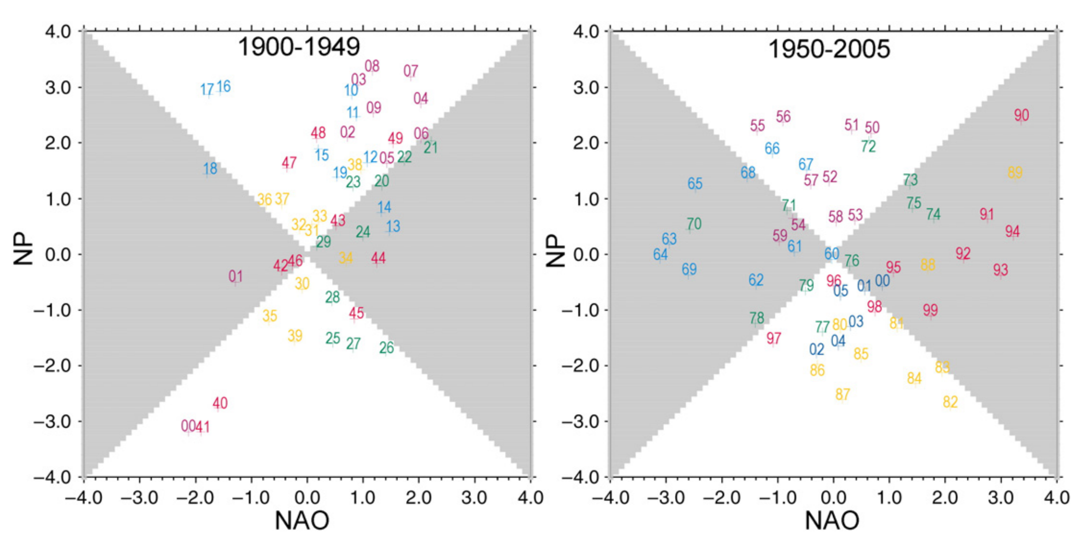

Fig. 5. Phase plot of the NAO and the NP indices, from www.cgd.ucar.edu/cas/jhurrell/indices.html. The Icelandic Low is deep when the NAO is positive and the Aleutian Low is deep when the NP is minus. There is a 3-year running mean on the data.

direction, other times when climate forcing of Atlantic and Pacific ecosystems is out of phase or decoupled.

To illustrate this point, we assess the relative importance of the Atlantic and Pacific climate patterns by plotting the winter NAO versus NP indices (Fig. 5). This gives a phase plot representing the state of the climate in any winter (listed as years for the 20th century). Given the scatter of points and the nearly equal distributions in all four quadrants, there is no clear indication of coordinated weather patterns between the North Pacific and North Atlantic. As the Pacific variability is more interdecadal and the Atlantic is more decadal, there are periods when the two do lie in the same quadrant. From 1950–2000 there is a trend toward lower NP SLP as the NAO is positive in the 1990s and negative in the 1960s, while the NP SLP was high in the 1950s and low in the 1980s. From 1903 to mid-1920s the NAO was mostly positive and the Aleutian Low was weak (High NP index). Therefore, while there appears to be no systematic covariability between the Atlantic and Pacific over the entire 20th century, there are decadal periods where the state of the climate in the same region is in phase. One time is the 1980s when both the Icelandic Low (NAO +) and Aleutian Low pressures were low (NP-) There could be some reinforcement of the Atlantic pattern by the Pacific in this period (Honda and Nakamura, 2001). Unusual conditions in the past decade are shown by both indices lying near the origin, suggesting that neither index explains recent climate variability. The 1930s was also a time when both indices were small.

2.2. An analysis of global teleconnections based on SLP

To extend this comparison of the North Pacific and North Atlantic teleconnections globally, we present a common dynamic factor analysis of SLP at 23 high and low pressure centers worldwide (Fig. 6). This analysis shows the connectivity between the dominant SLP centers over the past century, and reveals how the climate forcing of ecosystems co-varies in space and time.

The quarterly time series (1899–2001) were derived from the 5° global SLP data set from Minobe (1999). Each series was decomposed into a non-parametric trend (i.e. a time-varying mean), a non-stationary seasonal term, a stochastic cycle (with changing phase and amplitude) and observation error (Harvey, 1989; Durbin and Koopman, 2001). "Common trends" were then calculated by removing the seasonal and cyclic terms and using a subspace identification algorithm (Larimore, 1983; Aoki, 1990; Favoreel et al., 1998) to calculate a reduced (in the dimension of the state vector of the model) representation of the resulting series. "Common seasonals" and "common cycles" can be calculated analogously. Similar to PCA or EOF analysis, the purpose is to identify distinct regions that display common climate variability over time. The decomposition and common dynamic factor methods are described fully in Mendelssohn and Schwing (1997) and Mendelssohn et al. (2003), and can be performed on any physical or biological variable.

The first common factor for the trend components of the SLP time series (not shown) describes the mean level for SLP at each site, much like the leading mode of a PCA often does. A cluster analysis of the next three modes reveals atmospheric teleconnections that link ecosystems globally. Locations that cluster statistically are shown in the same color in Fig. 6 (upper panel). Similar shades (i.e., blues, yellow/orange) have a closer affinity than contrasting colors. SLP clusters in the eastern Pacific (dark blue) have a similar temporal pattern of variability and are loosely connected to SLP over Asia (light blue). Low pressure centers in the western end of the SO cluster (yellow), with some connection to the PNA area (orange) and another region extending from North America across the Atlantic (red). SLP trend variations forcing the CCS and HCS are not strongly teleconnected with either the Kuroshio/Oyashio Current Systems or the Aleutian Low

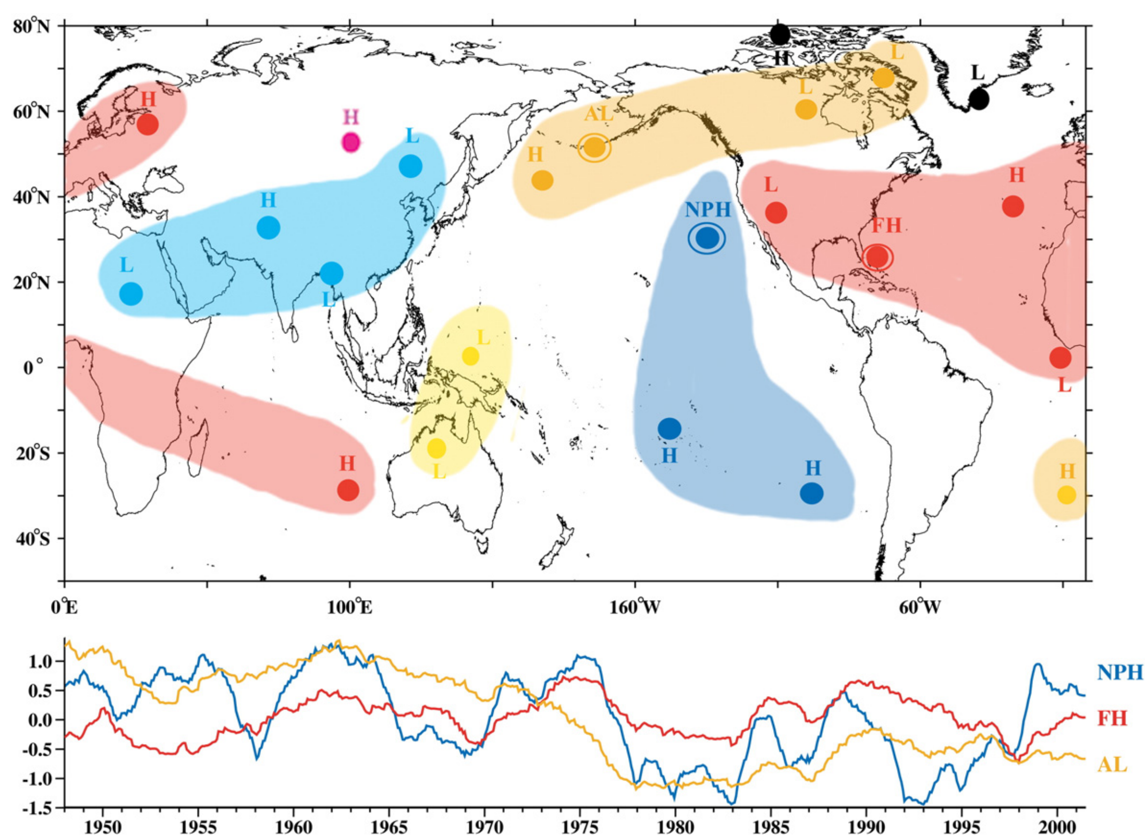

Fig. 6. Cluster analysis of SLP common trends 2–4, quantifying the relationship between 23 dominant sea level pressure (SLP) centers (shown in map, at top). Locations that cluster statistically, based on the behavior of their time series, are shown in the same color. Time series for North Pacific High (NPH), Florida High (FH), and Alaskan Low (AL), lower panel, are representative of the temporal tendencies for their respective geographic clusters. Locations are shown on the map.

over the GOA on the decadal scales identified in this analysis. Communication between the Pacific and Atlantic is via high-latitude teleconnections. SLP variability in the Arctic and the Icelandic Low does not share a temporal pattern with the other regions.

The lower panel of Fig. 6 shows representative time series of the trend clusters from the North Pacific High (NPH), the Aleutian Low (AL), and the Florida High (FH), with the first common factor removed. Regime shifts identified in previous studies (1976, 1989, 1998) can be seen in some or all of the series, although their abruptness and timing differs. The North Pacific High displays larger and more abrupt decadal variations than the other locations. Visually the Aleutian Low varies more like the Florida High than the North Pacific High, as their clustering indicates. However, there are still significant differences between the Aleutian Low and the Florida High, in particular near the 1970s regime shift.

The eastern Pacific is connected across the equator, so the HCS and CCS ecosystems experience strong correlated decadal climate forcing by the atmosphere. While the eastern and western Pacific are coupled on ENSO scales, the variance identified with this analysis selects decadal variability, which is not teleconnected zonally in the tropical Pacific. The eastern Pacific LMEs also are not teleconnected with the LMEs in the Northwest and subarctic Pacific. The conclusion from this analysis is that the eastern and western edges of the Pacific are not coupled via direct atmospheric forcing on climate time scales.

3. Pacific LMEs — the physical setting

While teleconnections link climate variability between distant ecosystems, populations respond to more immediate influences. It is the interaction between regional to basin-scale climate forcing and processes and factors at the ecosystem (and sub-ecosystem) level that determine how marine ecosystems are impacted by climate variability. In this section, we identify the principal features and processes in each Pacific coastal LME that force marine populations and are sensitive to climate variability. The purpose of this overview is to define a limited set of factors that are most strongly related to climate change and drive ecosystem variability.

Table 1 identifies the primary ocean features and processes in several Pacific LMEs. These physical attributes not only are key in driving ecosystem structure and production, but also sensitive to climate variability on a wide range of time and space scales. The EBCs are known to be particularly sensitive to interannual to decadal variability, but new information indicates that the physics, chemistry, and biology of all LMEs display some level of natural variability on these longer time scales. Further, recent results substantiate the idea that ecosystems do not respond uniformly to global climate variability. Certain areas *within* these ecosystems appear more sensitive to climate forcing, due to the interaction of global signals to local topography and coastal morphology, freshwater inflow and buoyancy, etc. (Parrish et al., 1983; Schwing and Mendelssohn, 1997a,b; Mendelssohn and Schwing, 2002).

3.1. Eastern boundary current LMEs

The California and Humboldt Current Systems, like other EBCs, are characterized by a broad, complex equatorward surface flow, fed by a broad zonal current entering the coastal region at a high latitude, interacting with the coastal upwelling and its offshore flowing filaments (Hill et al., 1998; Hickey, 1998; Strub et al., 1998; PICES, 2004). This flow is part of a basin-wide anti-cyclonic (clockwise in the Northern Hemisphere) circulation that enters each system from the west at mid-latitude (35–45°N). It transports sub-polar water with a distinct low temperature and salinity, and high dissolved oxygen and nutrient signature. A poleward subsurface current, which surfaces in certain locations and seasons, transports sub-tropical water with a clear contrasting signal to the equatorward flow.

Within this simplistic image of EBC circulation are numerous countercurrents, eddies and meanders on scales 10–500 km that may be exploited by populations, but complicate our understanding and modeling of the systems' transport and flux. The dominant process that controls much of the sub-ecosystem transport and water column structure, as well as biological processes, is coastal upwelling – driven by equatorward wind stress in association with a high pressure system over the ocean to the west – and the related offshore upwelling associated with the Ekman pumping due to positive wind stress curl. Generally, high production of zooplankton and small pelagic fish (e.g. sardine, anchovy, etc.) is supported by upwelling systems. The seasonal onset of upwelling in EBCs is important in setting the annual biological productivity and breeding success for many species (Schwing et al., 2006). Coastal capes and headlands and, in the CCS, deep submarine canyons that transect the continental shelf, contribute to local upwelling "hot spots" and much of the complex coastal circulation. Upwelling filaments can transport water and material well offshore. Freshwater input to these EBCs is limited to a few rivers, whose flow is predominantly in later winter and spring.

In addition to the atmospheric teleconnections described above, ocean remote forcing from lower latitudes, including the equatorial Pacific, is via coastal Kelvin waves. These are particularly evident during El Niño years (Enfield and Allen, 1980), but are thought to be restricted at latitudes poleward of about 40° (Clarke and Van Gorder, 1994). Because of its proximity to the equator, the HCS typically is influenced more strongly by Kelvin waves originating in the equatorial Pacific. Both systems appear to be strongly influenced by decadal climate availability as well; e.g. as characterized by the PDO.

3.2. Western boundary current LMEs

On the opposite side of the basin, the Kuroshio and Oyashio Systems are western boundary currents (WBCs) within the subtropical and subarctic circulation gyres of the North Pacific, respectively (Stommel and Yoshida, 1972). The principal feature of the Kuroshio is its strong poleward meandering flow. While the Kuroshio is low in nutrients, the Oyashio brings nutrient-rich water into the region, resulting in high productivity where the two currents confluence. Although the Kuroshio is a classic WBC, it is unique in its interaction with semi-enclosed seas along its coastal boundary and the unusual bimodal oscillation of its path. Its coastal region is predominantly downwelling, although topographically-driven upwelling occurs off the shelf. The Oyashio is fed by water from the Sea of Okhotsk and the Alaskan Stream, and indirectly via the East Kamchatka Current out of the Bering Sea. The outflow of the Kuroshio, the Kuroshio Extension, feeds into the North Pacific Current, while the outflow from Oyashio feeds into the Subarctic Current. Between these two eastward flows, the Transition Domain is formed (Favorite et al., 1976).

Like the EBCs, small pelagic fish utilize inshore areas of high production and offshore warm temperature in the KCS. One of the distinctive contrasts of the small pelagic fish in the Kuroshio–Oyashio system is their large migration (Ito et al., 2004). They mainly spawn in the subtropical region and migrate to subarctic waters to feed in the highly productive subarctic region. The dominant zooplankton size increases with latitude, and the start of active plankton production is early in the south and later in the north. This suggests that ontogenetic horizontal migration of these pelagic fish is consistent with the "surf riding theory", where seasonal reproduction occurs on time and space scales to take advantage of the "wave" of food supply (Pope et al., 1994).

3.3. Subarctic LME

At higher latitudes, the Gulf of Alaska System is a downwelling-favorable system that is heavily influenced by high freshwater input along its coastal boundary, and a cyclonic circulation that is fed from the south by the same North Pacific Current that bifurcates into the CCS (Royer, 1998; PICES, 2004; King, 2005; Royer, 2005; Royer and

Table 1
Summary of features in Pacific LMEs that are important to ecosystem structure and production.

Feature	CCS	HCS	GOA	K/O CS
Source of atm forcing	North Pacific High	South Pacific High/ITCZ	Aleutian Low	North Pacific High (K)/Aleutian Low (O)
Source of water	North Pacific Current (40–45°N)	West Wind Drift (35–45°S)	North Pacific Current (45–50°N)	North Equatorial Current (10–15°N/Alaskan Stream (50°N) and marginal seas
Source water properties	Low T, S; high nut, O^2	Low T, S, O^2; high nut	Low T, S; high nut, O^2	High T, S; low nut (K)/Low T, S; high nut (O)
Boundary current	California Current (max summer), equatorward meandering, local jets	Peru Current (equatorward offshore), poleward/mixed inshore	Alaskan Stream; western boundary current	Kuroshio (strong poleward)/Oyashio (strong equatorward) and Tsugaru Current
Undercurrent/ countercurrent	California Undercurrent/Davidson Current (winter)	Peru/Chile Countercurrent (offshore); poleward undercurrent (summer–fall)		
Outflow of boundary current	North Equatorial Current (20–30°N)	South Equatorial Current (0–10°N)	Alaskan Stream (50°N)	Kuroshio Extension/North Pacific Current (30–45°N)
Topography	Narrow shelf, canyons, capes, So Cal Bight	Narrow shelf, capes	Variable width shelf, numerous rivers, bays, canyons	Narrow shelf, marginal seas
Biogeographical boundaries	Pt. Concepcion, Cape Mendocino	Southern Peru, Central Chile, Pta. Lavapie	Shelf/offshore, Aleutian Is.	Kuroshio Extension Front
Freshwater input	Columbia River (7300 m^3/s); San Francisco Bay estuary	Bio–Bio River (1200 m^3/s in winter)	Large input (23,000 m^3/s), numerous sources	Yangtze, Yellow, Amur Rivers through marginal seas
Coastal wind stress/ upwelling	Southward (strong summer); coastal upwelling (year-round), curl pumping	Northward; strong coastal upwelling, (year-round), curl pumping offshore	Westward; downwelling (year-round)	Westward; downwelling (K)/weak (O) upwelling by Ekman pumping
Watershed precipitation	Arid (south), high winter (north)	Arid	Very high	High
Stratification	High near coast (upwelling), high (So CA Bight), mixed (winter)	High (Chile Basin)	Well mixed (winter)	Low (K)/High (O)
Ocean fronts	Ubiquitous thermal fronts		Numerous buoyancy (FW inflow) fronts	Kuroshio Extension Front/Oyashio (Subarctic) Front and Subarctic boundary
Ocean Kelvin/ Rossby waves	CTW/Remote Kelvin/westward Rossby field	CTW/remote Kelvin/Rossby field	Westward Rossby waves in Gulf	Rossby waves (from offshore)
Eddies/meanders	Strong meandering of main current; strong mesoscale eddy field	Filaments	Long-lived warm eddies advect westward	Cold rings from Oyashio/Warm core from Kuroshio Extension, downstream meanders
Spring transition/bloom	Onset of upwelling (Apr–May)		Onset of stratification (early summer)	Onset of stratification
Time scale				
Interannual	Strong— atm/ocean teleconnections, ENSO	Very strong— ocean teleconnections, ENSO	Moderate— atm teleconnection	Moderate— atm teleconection
Decadal	Strong— atm/ocean; multi-decadal regime shifts	Regime shifts	Strong— atm (PNA, AO), 18.6-yr tide; multi-decadal regime shifts	Barotropic response and Ocean and Rossby waves, 18.6-yr tide

Grosch, 2006). The westward Alaskan Stream accelerates as it flows toward the Aleutian Islands. Large eddies emanating from off of British Columbia transit west along the Alaska shelf, and mesoscale eddies develop within the Stream. Both are thought to be nutrient-rich sources for production, survival and recruitment. Eddies, flow in submarine canyons and vigorous storm systems with west wind bursts are particularly important episodic processes that overcome the coastal downwelling climatology to transport the nutrients into the coastal zone. In the Bering Sea, sea ice plays an important role in structuring ecosystems (Hunt et al., 2002). In ice-covered areas, benthic food webs predominate, while in subarctic regions energy transfer is primarily within the pelagic zone. Unlike temperate Pacific LMEs, the GOA is usually well-mixed to 100–200 m, especially in winter. While ENSO signals occasionally affect this system, variability is dominant on the 18.6-year tidal period and on the same scales seen throughout the Pacific.

3.4. Climate impacts in LMEs and their mechanisms

Many of the features and processes controlling the environment of these LMEs (Table 1), as well as their populations, fluctuate on the scales that characterize climate variability. In this section, we summarize the primary processes responsible for variability on climate time scales in each of the LMEs considered here, and the physical features that are responsive to them (PICES, 2004, and citations therein). From this, common forcings and responses between these systems can be matched, one criterion for determining possible synchrony between populations.

Climate variability in the CCS is manifested through a number of processes, including: i) changes in local wind forcing, resulting in variations in coastal upwelling and offshore Ekman pumping; ii) changes in the transport of the California Current and California Undercurrent; iii) changes in source water properties and entry points; iv) volume and timing of freshwater input, particularly near the Columbia River and San Francisco Bay; v) changes in the mesoscale energy associated with eddies, fronts, and upwelling plumes; vi) remote forcing via atmospheric and oceanic teleconnections, most often associated with El Niño events; and vii) heating of the upper ocean by global atmospheric warming.

Principal processes displaying climate variabilities in the HCS are: i) strong coupling with equatorial ENSO signals from the atmosphere and ocean, leading to warmer water, higher coastal sea level (CSL), stronger poleward flow, deeper thermocline, and southward Inter-Tropical Convergence Zone (ITCZ) shift); ii) low latitude sensitivity of upwelling and Ekman processes to winds; iii) coastal trapped waves; iv) movement and strength of South Pacific High, ITCZ, and Polar Front; v) position of South Pacific convergence zone; and vi) global warming.

There has been a great deal of synchrony in the eastern Pacific Ocean between the CCS and HCS in the past, both physically (Schwing and Mendelssohn, 1997b) and biologically (Lluch-Belda et al., 1992). Climate variability on interannual and decadal scales also is similar in both the North and South Pacific. Since these LMEs share many dominant physical features and processes (e.g., coastal upwelling, ENSO), there is a mechanistic as well as correlative rationale for expecting a synchrony in the variability of their populations. Since coastal upwelling is the dominant process in the HCS and CCS, it is likely that both systems may have a similar response to climate variability that influences this process. However, the HCS is more sensitive to ENSO processes and its coastal impacts, while decadal regime shifts appear to play a greater role in CCS variability.

Climate variability in the GOA is due principally to: i) variations in precipitation and freshwater input; ii) ENSO, through atmospheric teleconnections; iii) decadal fluctuations in the Aleutian Low; iv) changes in Ekman transport and coastal and ocean upwelling/downwelling, due to wind stress variability; v) adjustments in MLD and pycnocline depth due to variability in the strength of the basin winds (mixing and Ekman processes) and subarctic gyre; vi) strength of the Alaskan Stream, for the same reasons; vii) global warming heating of the upper ocean, which is relatively greater at higher latitudes, viii) mesoscale eddies, due to the strength of coastal current; and ix) input via Sitka, Haida, and Juan de Fuca eddies.

Variability in the GOA and CCS is primarily in the form of interannual events and multi-decadal climate regimes alternating between high and low production (Mantua et al., 1997; Peterson and Schwing, 2003). The GOA, like the CCS and HCS, is impacted by ENSO. The North Pacific systems are more influenced by atmospheric teleconnections, while direct interannual ocean forcing from ENSO dominates in the southeastern Pacific (Strub et al., 1998). The GOA and CCS share some variability due to long-term fluctuations in atmospheric forcing of the Northeast Pacific.

In the KCS, climate variability is due primarily to: i) decadal fluctuations in the North Pacific subtropical gyre; ii) interannual shifts in the Kuroshio Current meander path; iii) vorticity adjustments of the path related to the Current's transport; iv) lateral ocean heat divergence due to wind stress curl, which alters SST and subsequently air–sea heat flux; and v) ocean Rossby waves surfacing temperature and salinity anomalies into the region, which affect SST anomalies, volume of transport, nutrient availability by lateral advection and upwelling into the mixed layer, mesoscale eddy variability, and the meandering of the Kuroshio Current path.

Climate variability in OCS is due to: i) wind stress changes associated with the Aleutian Low; ii) Rossby wave propagations; iii) upstream Western Subarctic Gyre (WSAG) and Okhotsk Sea conditions; and iv) tidal mixing along the Kuril Islands.

The dominant climate variability in the GOA and western North Pacific is decadal, but from different sources. Much of the variability in the KCS is via remotely generated ocean Rossby waves that may create a lag in the response compared to the eastern LMEs. Variations in the strength of the Aleutian Low can be decomposed to bi-decadal and penta-decadal oscillations (Minobe, 1999), but only the penta-decadal signal can survive to travel to the western boundary region (Tatebe and Yasuda, 2005). Moreover, many other local factors contribute to environmental variability in the Kuroshio/Oyashio LMEs, making it quite unlikely that these systems respond to the same climate forcing on the same time frame as those in the east. Thus, observed synchrony between their populations may be coincidental.

The Kuroshio Extension is the most dynamic region in the North Pacific with respect to sea surface height (SSH) and eddy variability and SST, and (next to equatorial Pacific) the largest heat-releasing source to the atmosphere. Decadal changes in the Kuroshio Current transport feed into the strength and position of the Kuroshio Extension and North Pacific Current, which eventually affect SST gradients, ocean heat transport, and the overlying atmosphere (Wang et al., 2004). These can contribute to changes in the CCS and GOA, but with a several year lag.

3.5. Synchrony of climate variability in Pacific LMES

To help project the synchrony of climate change and how it alters marine ecosystems, we can characterize the temporal and spatial nature of past climate variability and relate this to specific forces and mechanisms within LMEs. The common factor analysis is applied again to objectively examine synchronous SST variability within these ecosystems. These results provide an example of how LMEs may respond to climate variability, and lend insight on how future climate change may be manifested in a coherent or synchronous way. SST is one of several environmental drivers, and represents only near-surface conditions, not vertical temperature structure. However, it serves as a proxy for upper ocean state and much of the physical variability that directly drives population variability. SST is also

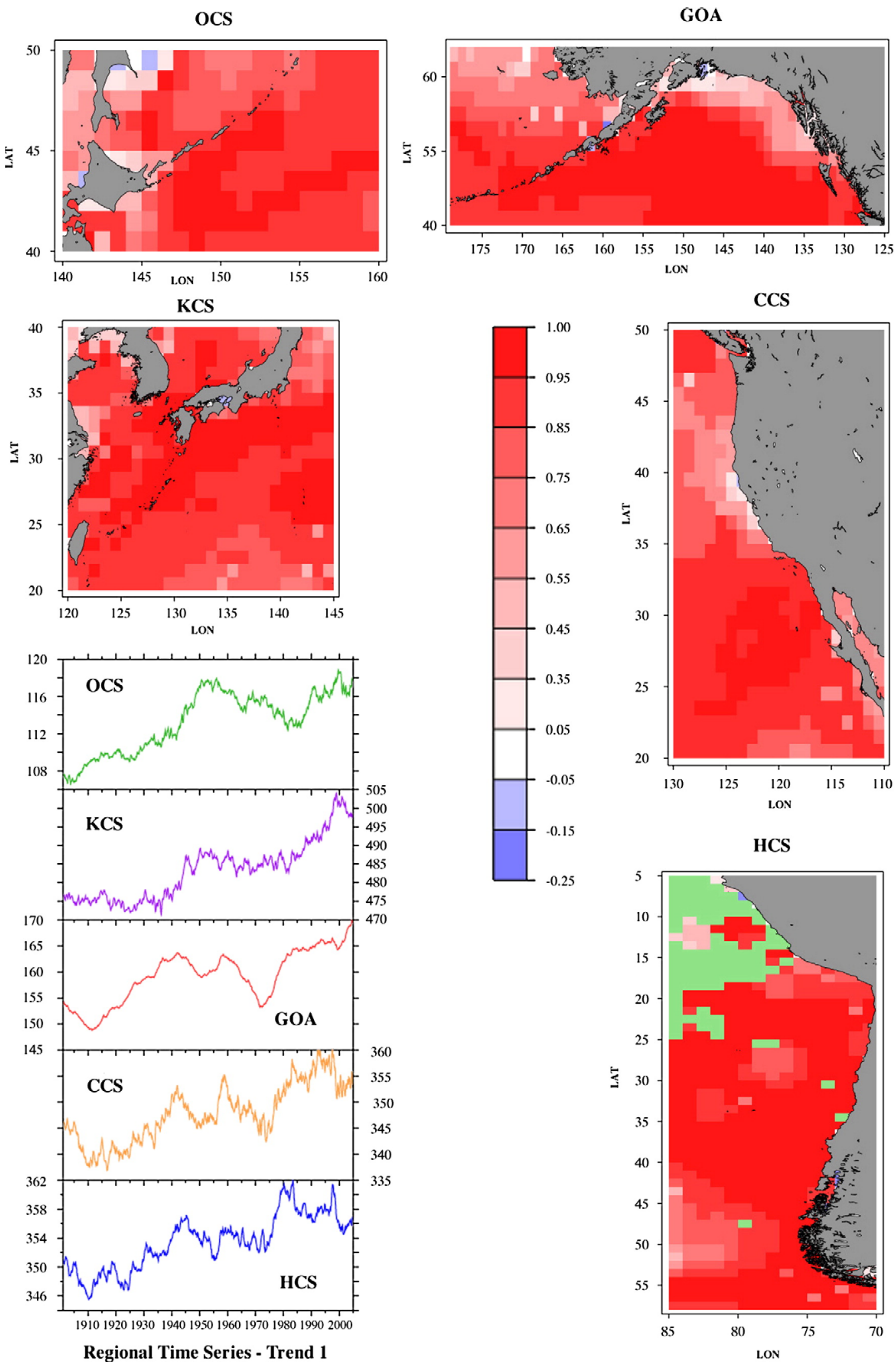

Fig. 7. Spatial correlations of the first SST common trend for each LME. Trend time series for each LME are shown in bottom left. The color bar denotes the magnitude of the spatial correlations on each map. When scaled by the factor loadings (not shown), the time series represent a change of roughly 1–2 °C over the length of the series. Green areas denote locations where the univariate analysis gives a constant trend, and are not included in the common trend analysis shown here.

relatively well sampled in space and time, and its observations have been relatively accurate over the long (100+ year) record.

This analysis was carried out for each LME, based on the 1° gridded monthly mean SST data from the UK Meteorological Office (Hadley Centre) for 1900–1993 and monthly mean Optimally Interpolated SST for the years 1994–2005 from the NOAA-CIRES Climate Diagnostics Center (http://www.cdc.noaa.gov). We present the leading two modes for each LME, to illustrate the dominant temporal variability over the previous century and the spatial patterns in each region, as well as the correspondence between SST temporal variability in these LMEs. The results show some evidence of synchronicity across the LMEs, an important result in determining the likelihood that their disparate populations may be responding coincidently to a global climate signal.

The first common trend in each LME reflects a persistent warming tendency since 1900 (Fig. 7). The rate of warming is similar in each system, ca. 1–2 °C over the past 100 years (based on the product of the spatial loading values and the associated time series). However there is notable variation within each LME. Centennial warming in the CCS has been less in the coastal region where upwelling dominates, consistent with increased coastal upwelling due to stronger southward wind stress that has mitigated (but not overcome) the warming trend (Bakun, 1990; Schwing and Mendelssohn, 1997a,b). In the GOA, a similar reduced coastal warming tendency may be due to reduced downwelling (due to the same wind-forced process that causes greater upwelling in the CCS) or more freshwater runoff from the continent (Royer, 2005; Royer and Grosch, 2006). Warming in the HCS is less in the dominant upwelling region off Peru, also consistent with intensified coastal upwelling (Bakun, 1990; Schwing and Mendelssohn, 1997a,b). The green areas that predominate within 20° of the equator do not have a significant long-term trend as determined by state-space models, but are dominated by a SST cycle coinciding with ENSO.

Superimposed on the common factor 1 time series are multidecadal fluctuations that result in periods of more rapid and slower warming, and even episodes of cooling. Although superficially similar, these fluctuations do not reflect PDO variability. The correspondence in these intra-centennial fluctuations is very close in the eastern Pacific (GOA, CCS, HCS) with warming in the 1920s and 1930s, cooling in the 1940s and 1960s (with a lengthy warm period during and following the 1957–58 El Niño), and more rapid warming in the 1970s. This pattern is very similar to the global mean surface temperature record (Mann et al., 2000). Regional differences have dominated in the eastern Pacific since about 1980. While the SST tendency continued to increase in the GOA, the CCS shows a rapid cooling since about 1989, roughly when Beamish et al. (1999) and Hare and Mantua (2000) identified a regime shift. This is part of a longer-term cooling of the leading common factor in the HCS since about 1980. Thus, while there is much evidence that SST in the eastern Pacific LMEs has varied with the global SST trend, regional differences have occurred, particularly in recent decades.

Similar decadal-scale fluctuations in SST are evident in the western Pacific (Fig. 7). However the timing of these fluctuations lags the eastern Pacific by about a decade. It appears that SST, and perhaps other ocean conditions, in the Pacific LMEs are a combination of globally coherent and regionally specific signals. Subsurface temperature decadal variations in the western North Pacific lag those in the central part of the basin, and the wind stress curl thought to drive them, by about 5 years (Miller et al., 1998; Deser et al., 1999). Since the eastern and western North Pacific are less well-coupled and clearly not in phase, the biological response to climate variability between east and west is probably not synchronous either.

The second common trend in each LME (Fig. 8) reflects sub-ecosystem differences, and again shows a similar centennial temporal pattern — a general warming trend that rapidly accelerated in the latter half of the 20th century. This pattern is consistent with the entire North Pacific, as well as equatorial Pacific (Mendelssohn et al., 2005) and the long-term loss of Arctic ice coverage (Chapman and Walsh, 1993). As with the first common factor, there are notable differences between LMEs. In particular, an acceleration of the warming tendency began in the 1970s in the CCS, while there were two abrupt warming events in about 1975 and 2000 in the GOA. The warming acceleration in the HCS and the eastern Pacific did not start until about 1980.

The higher modes of the common dynamic factor analysis, as well as similar analyses on the seasonal and cycle components of the state-space models, reveal similar regional differences in SST variability over the past century (Mann et al., 2000). Thus global synchrony in climate forcing of distinct marine populations is modulated by different responses within each LME, which will reduce the correlation and synchrony between regime shifts and other multidecadal fluctuations.

4. Discussion

On a broad scale, ocean conditions in the coastal LMEs of the Pacific are driven by the basin-scale atmospheric pressure systems and their associated winds. Atmospheric teleconnections link distant regions to remote climate forcing. These large-scale atmospheric forces establish the large ocean circulation gyres, notably the North Pacific Subtropical and Subarctic gyres in the North Pacific and the South Pacific gyre, but also the coastal currents that influence key ecosystem processes such as upwelling, cross-shelf exchange, and mixing. Freshwater input to the coastal ocean is important in some regions and systems (particularly the GOA). The interaction of the coastal currents with steep or irregular coastlines and bathymetry is another important factor. Heat flux into the atmosphere is particularly important at higher latitudes. Finally, internal ocean processes, most notably Kelvin and Rossby waves, influence remote ocean as well as atmospheric conditions.

Global climate signals are not manifested equally in coastal LMEs. Atmospheric teleconnections and ocean gyres and planetary waves transmit climate signals over large distances, but these signals are modulated by local and regional factors, which disrupt and shift the timing and relative significance of their impacts on ecosystem and sub-ecosystem scales. The resulting interannual and longer variability will have regional and local differences between and within ecosystems. These differences will be exacerbated if disparate systems do not share dominant features and processes controlling their ecosystems. Thus the correspondence of common trends in SST (Figs. 7, 8) and other critical physical variables provides vital insight not only into the time scales and spatial patterns of climate variability in each LME, but also into the sources of such variability and the likelihood of synchronous climate forcing and ecosystem response between comparable systems.

Since the factors summarized in Table 1 set the mean and seasonally-varying physical conditions, and establish physical and biological patterns (e.g., advection, primary productivity) that determine the status of marine populations, LME populations will be responsive to variability in these factors on climate (interannual and longer) scales. The ocean response to climate variability is a combination of direct forcing on a number of space scales with internal ocean variability. For example, ENSO contributions to extratropical forcing are via atmospheric teleconnections on intraseasonal and longer scales as well as coastal Kelvin waves. Decadal variability in the North Pacific is thought to be driven by internal ocean Rossby waves generated in the eastern Pacific, which propagate freely across the basin before their signals surface in the Kuroshio region a decade later (e.g., Jacobs et al., 1994; Miller et al., 1998; Qiu, 2003). A spin-up of the large-scale circulation alters the input of source water to these coastal ecosystems, but also leads to adjustments in vertical transport and pycnocline depth and strength, heat

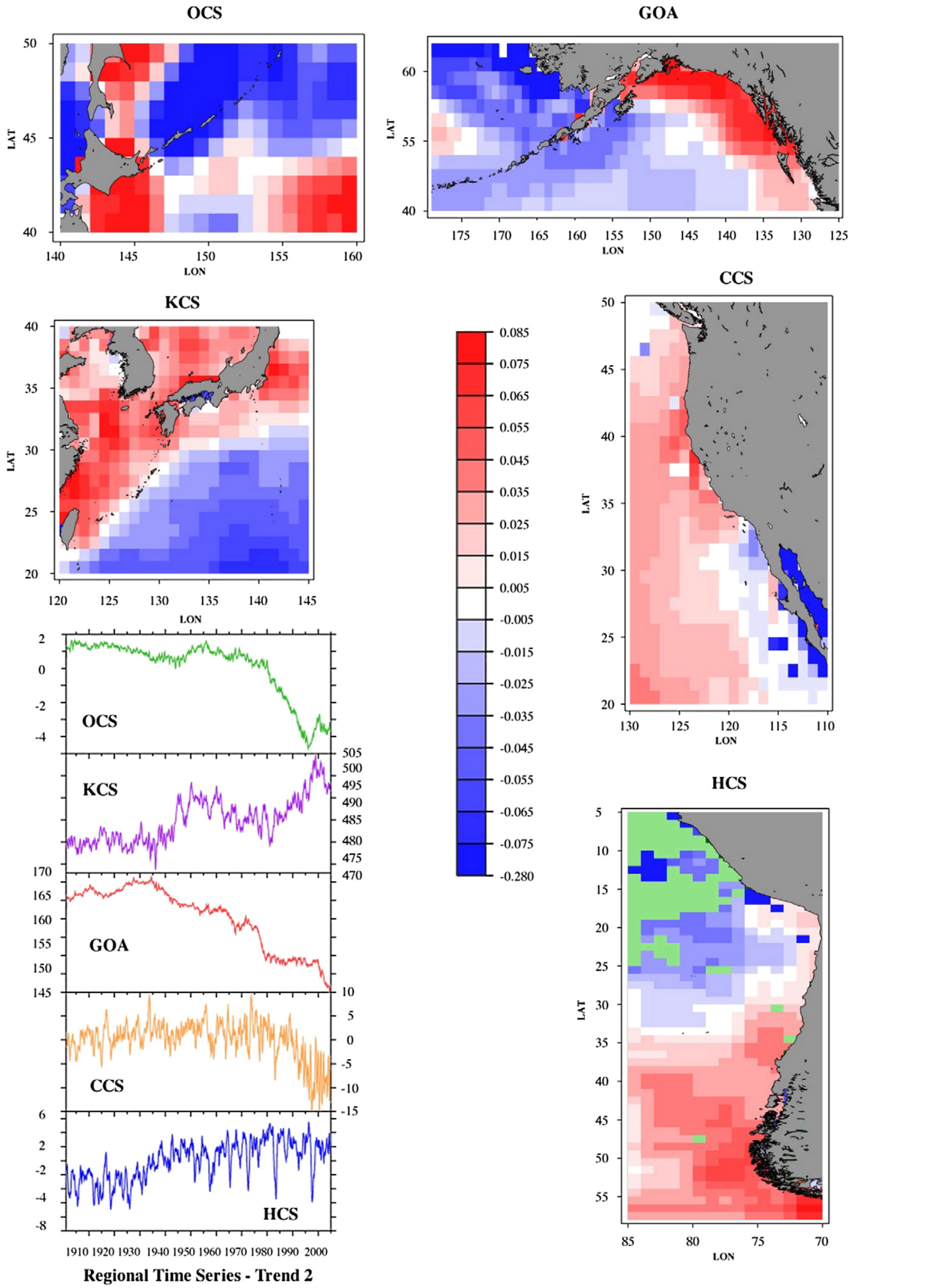

Fig. 8. Spatial loadings of the second SST common trend for each LME. Trend time series for each LME are shown in bottom left. The color bar denotes the magnitude of the spatial loadings on each map. Multiplying these by the values of the time series gives the magnitude of the SST for this common trend for each time and location. Green areas denote locations where univariate analysis gives a constant trend, and are not included in the common trend analysis shown here.

exchange with the atmosphere, and ultimately affect coastal weather patterns (altered winds, precipitation and runoff patterns, etc.) (McPhaden and Zhang, 2004).

Beyond the general global coherence of climate's impacts on the oceans, regions that have common physical features and processes (Table 1) are likely to share a comparable response to climate change. The LMEs of the eastern and western Pacific have many physical dissimilarities. The types of forcing and processes also have little in common. Because the key processes in the eastern and western coastal LMEs differ, it is likely that the regional response to common global forcing may be different, but occur on the same time scales. There is less evidence that the same sources of atmospheric forcing impact the eastern and western regions of the North Pacific. Atmospheric variabilities in the CCS and HCS regions share a common dynamic not seen in the Kuroshio/Oyashio regions (Fig. 6). One possible climate connection may be via ocean Rossby waves propagating across the basin (Jacobs et al., 1994), but there is a several year lag between their generation and their arrival in the WBC region (Deser et al., 1999; Miller and Schneider, 2000). ENSO-generated atmospheric anomalies that lead to extra-tropical ocean changes in the eastern Pacific may also be linked to changes in the subtropical western Pacific atmosphere (Alexander et al., 2002). However, at present it is uncertain how much this impacts the Kuroshio/Oyashio region. Therefore, it is reasonable to expect that climate variability does not affect the KC/OC and CCS/HCS similarly.

Past synchrony between disparate populations may be coincidental. Due to our short observational record, we cannot confirm what is due to climate variability, and has a synchronous physical response within and between LMEs. Analyses such as those described here, and the biologically-relevant indices that are developed from them, are useful for summarizing large volumes of data. However, they can be problematic. Analyses force data into modes with limitations. The results may be weighted or biased to certain geographical areas remote from areas to which they are applied. Indices may be proxies, but not true mechanisms of climate impacts. The “filters” used by scientists to interpret and synthesize observations into information about climate variability – whether objective or intuitive – are based on how we perceive the ocean, and are not necessarily those used by marine populations to “see” their environment.

While basin- to global-scale atmospheric forcing is the initial driver of ocean variability in all of the LMEs considered here, the processes key to each system (Table 1) modify large-scale climate signals, giving each region and its populations a unique pattern of climate variability. The spatial patterns and timing – and impacts – of this variability will vary geographically, reducing the likelihood that disparate populations will vary synchronously. Much more work on understanding the mechanisms linking physical climate change to marine ecosystems is needed to determine how coastal marine populations react to their environmental variability, and to forecast the likely response of these populations to the pressures of future climate change.

Acknowledgments

This publication is supported in part by the US GLOBEC Program, Contribution #622, and partially funded by the Joint Institute for the Study of the Atmosphere and Ocean (JISAO) under NOAA Cooperative Agreement No. NA17RJ1232, Contribution #1742. The co-author SI was supported in part by the Japanese Society for Promotion of Science (Grant-in-aid for scientific research (B), No. 19340140).

References

Alexander, M.A., Bladé, I., Newman, M., Lanzante, J.R., Lau, N.-C., Scott, J.D., 2002. The atmospheric bridge: the influence of ENSO teleconnections on air–sea interaction over the global oceans. J. Climate 15, 2205–2231.

Alexander, M.A., Lau, N.-C., Scott, J.D., 2004. Broadening the atmospheric bridge paradigm: ENSO teleconnections to the North Pacific in summer and to the tropical west Pacific–Indian Oceans over the seasonal cycle. In: Wang, C., Xie, S.-P., Carton, J. (Eds.), Earth Climate: The Ocean–Atmosphere Interaction. AGU Monograph, Washington, DC, pp. 85–104.

Alheit, J., Bakun, A., 2010. Population synchronies within and between ocean basins: apparent teleconnections and implications as to physical–biological linkage mechanisms. J. Mar. Syst. 79, 267–285 (this issue).

Aoki, M., 1990. State-Space Modeling of Time Series, 2nd Edition. Springer-Verlag, Berlin.

Bakun, A., 1990. Global climate change and intensification of coastal ocean upwelling. Science 247, 198–201.

Barnston, A.G., Livezey, R.E., 1987. Classification, seasonality and persistence of low-frequency atmospheric circulation patterns. Mon. Weather Rev. 115, 1083–1126.

Beamish, R.J., Noakes, D., McFarlane, G.A., Klyashtorin, L., Ivonov, V.V., Kurashov, V., 1999. The regime concept and natural trends in the production of Pacific salmon. Can. J. Fish. Aquat. Sci. 56, 516–526.

Chapman, W.L., Walsh, J.E., 1993. Recent variations of sea ice and air temperatures at high latitudes. Bull. Am. Meteorol. Soc. 74, 33–47.

Clarke, A.J., Lebedev, A., 1999. Remotely driven decadal and longer changes in coastal Pacific waters of the Americas. J. Phys. Oceanogr. 29, 828–835.

Clarke, A.J., Van Gorder, S., 1994. On ENSO coastal currents and sea levels. J. Phys. Oceanogr. 24, 661–680.

Delcroix, T., Picaut, J., Eldin, G., 1991. Equatorial Kelvin and Rossby waves evidenced in the Pacific-Ocean through Geosat sea-level and surface current anomalies. J. Geophys. Res. 96, 3249–3262.

Deser, C., Alexander, M.A., Timlin, M.S., 1999. Evidence for a wind-driven intensification of the Kuroshio Current extension from the 1970s to the 1980s. J. Clim. 12, 1697–1706.

Durbin, J., Koopman, S.J., 2001. Time Series Analysis by State-Space Methods. Oxford University Press, Oxford.

Enfield, D.B., Allen, J.S., 1980. On the structure and dynamics of monthly mean sea level anomalies along the Pacific coast of North and South America. J. Phys. Oceanogr. 10, 557–578.

Favoreel, W., Sima, V., Van Huffel, S., Verhaegen, M., De Moor, B., 1998. Subspace model identification of linear systems in SLICOT. SLICOT Working Note #1998-6, Working Group on Software. Katholieke University, Leuven, Belgium. 29 pp.

Favorite, F., Dodimead, A.J., Nasu, K., 1976. Oceanography of the subarctic Pacific region 1960–71. Bull. Int. Nor. Pac. Fish. Comm. 33, 1–187.

Gu, D., Philander, S.G.H., 1997. Interdecadal climate fluctuations that depend on exchanges between the tropics and extratropics. Science 275, 805–807.

Hare, S.R., Mantua, N.J., 2000. Empirical evidence for North Pacific regime shifts in 1977 and 1989. Prog. Oceanogr. 47, 103–145.

Harvey, A.C., 1989. Forecasting, Structural Time Series Models and the Kalman Filter. Cambridge University Press.

Hickey, B.M., 1998. Coastal oceanography of western North America from the tip of Baja California to Vancouver Island. In: Robinson, A.R., Brink, K.H. (Eds.), The Global Coastal Ocean: Regional Studies and Synthesis. John Wiley and Sons, Inc., New York, pp. 345–394.

Hill, A.E., Hickey, B.M., Shillington, F.A., Strub, P.T., Brink, K.H., Barton, E.D., Thomas, A.C., 1998. Eastern Ocean boundaries. In: Robinson, A.R., Brink, K.H. (Eds.), The Global Coastal Ocean: Regional Studies and Synthesis. John Wiley and Sons, Inc., New York, pp. 29–67.

Honda, M., Nakamura, H., 2001. Interannual seesaw between the Aleutian and Icelandic lows. Part II: its significance in the interannual variability over the wintertime Northern Hemisphere. J. Climate 14, 4512–4529.

Horel, J., Wallace, J.M., 1981. Planetary-scale atmospheric phenomena associated with the Southern Oscillation. Mon. Weather Rev. 109, 813–829.

Hunt Jr., G.L., Stabeno, P., Walters, G., Sinclair, E., Brodeur, R.D., Napp, J.M., Bond, N.A., 2002. Climate change and control of the southeastern Bering Sea pelagic ecosystem. Deep-Sea Res. II 49, 5821–5853.

Hurrell, J.W., 1996. Influence of variations in extratropical wintertime teleconnections on Northern Hemisphere temperature. Geophys. Res. Lett. 23, 665–668.

Ito, S., Sugisaki, H., Tsuda, A., Yamamura, O., Okuda, K., 2004. Contributions of the VENFISH program: meso-zooplankton, Pacific saury (*Cololabis saira*) and walleye pollock (*Theragra chalcogramma*) in the northwestern Pacific. Fish. Oceanogr. 13 (Suppl. 1), 1–9.

Jacobs, G.A., Hurlburt, H.E., Kindle, J.C., Metzger, E.J., Mitchell, J.L., Teague, W.J., Wallcraft, A.J., 1994. Decade-scale trans-Pacific propagation and warming effects of an El Niño anomaly. Nature 370, 360–363.

King, J.R. (Ed.), 2005. Report of the Study Group on the Fisheries and Ecosystem Responses to Recent Regime Shifts. PICES Scientific Report No. 28.

Klein, S.A., Soden, B.J., Lau, N.-C., 1999. Remote sea surface temperature variations during ENSO: evidence for a tropical atmospheric bridge. J. Climate 12, 917–932.

Larimore, W.E., 1983. System identification, reduced-order filtering and modeling via canonical variate analysis. In: Rao, H.S., Dorato, T. (Eds.), 1983 American Control Conference. IEEE, New York, pp. 445–451.

Lau, N.-C., 1997. Interactions between global SST anomalies and the midlatitude atmospheric circulation. Bull. Am. Meteor. Soc. 78, 21–33.

Lluch-Belda, D., Schwartzlose, R.A., Serra, R., Parrish, R., Kawasaki, T., Hedgecock, D., Crawford, R.J.M., 1992. Sardine and anchovy regime fluctuations of abundance in four regions of the world oceans: a workshop report. Fish. Oceanogr. 1, 339–347.

Lynn, R.J., Schwing, F.B., Hayward, T.L., 1995. The effect of the 1991–1993 ENSO on the California Current System. Calif. Coop. Ocean. Fish. Investig., Data Rep. 36, 57–71.

Mann, M.E., Gille, E.P., Bradley, R.S., Hughes, M.K., Overpeck, J.T., Keimig, F.T., Gross, W.S., 2000. Global temperature patterns. Past Centuries: An Interactive Presentation, IGBP Pages/World Data Center for Paleoclimatology Data Contribution Series #2000-075. NOAA/NGDC Paleoclimatology Program, Boulder CO.

Mantua, N.J., Hare, S.R., Zhang, Y., 1997. A Pacific interdecadal climate oscillation with impacts on salmon production. Bull. Am. Meteor. Soc. 78, 1069–1079.

McFarlane, G.A., King, J.R., Beamish, R.J., 2000. Have there been recent changes in climate? Ask the fish. Prog. Oceanogr. 47, 147–169.
McPhaden, M.J., Zhang, D., 2004. Pacific Ocean circulation rebounds. Geophys. Res. Lett. 31. doi:10.1029/2004GL020727.
Mendelssohn, R., Schwing, F.B., 1997. Application of state-space models to ocean climate variability in the northeast Pacific Ocean. In: Aoki, M., Havenner, A.M. (Eds.), Applications of Computer-Aided Time Series Modeling, Lecture Notes in Statistics, vol. 119. Springer, New York, pp. 255–280.
Mendelssohn, R., Schwing, F.B., 2002. Common and uncommon trends in SST and wind stress in the California and Peru–Chile Current Systems. Prog. Oceanogr. 53, 141–162.
Mendelssohn, R., Schwing, F.B., Bograd, S.J., 2003. Spatial structure of subsurface temperature variability in the California Current, 1950–1993. J. Geophys. Res. 108, 3093. doi:10.1029/2002JC001568.
Mendelssohn, R., Schwing, F.B., Bograd, S.J., 2004. Nonstationary seasonality of upper ocean temperature in the California Current. J. Geophys. Res. 109, C10015. doi:10.1029/2004JC002330.
Mendelssohn, R., Bograd, S.J., Schwing, F.B., Palacios, D.M., 2005. Teaching old indices new tricks: a state-space analysis of El Niño related climate indices. Geophys. Res. Lett. 32, L07709. doi:10.1029/2005GL022350.
Miller, A.J., Schneider, N., 2000. Interdecadal climate regime dynamics in the North Pacific Ocean: theories, observations and ecosystem impacts. Prog. Oceanogr. 47, 355–379.
Miller, A.J., Cayan, D.R., White, W.B., 1998. A westward-intensified decadal change in the North Pacific thermocline and gyre-scale circulation. J. Clim. 11, 3112–3127.
Minobe, S., 1999. Resonace in bidecadal and pentadecadal climate oscillations over the North Pacific: role in climatic regime shifts. Geophys. Res. Lett. 26, 855–858.
Mo, K.C., Hakkinen, S., 2001. Decadal variations in the tropical south Atlantic and linkages to the Pacific. Geophys. Res. Lett. 28, 2065–2068.
Namias, J., 1959. Recent seasonal interactions between North Pacific waters and the overlying atmospheric circulation. J. Geophys. Res. 64, 631–646.
Namias, J., 1969. Seasonal interactions between the North Pacific Ocean and the atmosphere during the 1960s. Mon. Weather Rev. 97, 173–192.
Newman, M., Compo, G.P., Alexander, M.A., 2003. ENSO-forced variability of the Pacific Decadal Oscillation. J. Climate 16, 3853–3857.
Overland, J.E., Wang, M., 2005. The Arctic climate paradox: the recent decrease of the Arctic Oscillation. Geophys. Res. Lett. 32, L06701. doi:10.1029/2004GL021752.
Overland, J.E., Percival, D.B., Mofjeld, H.O., 2006. Regime shifts and red noise in the North Pacific. Deep-Sea Res. I 53, 582–588.
Pares-Sierra, A., O'Brien, J.J., 1989. The seasonal and interannual variability of the California Current System: a numerical model. J. Geophys. Res. 94, 3159–3180.
Parrish, R.H., Bakun, A., Husby, D.M., Nelson, C.S., 1983. Comparative climatology of selected environmental processes in relation to eastern boundary current fish production. FAO Fish. Rep. 291, 731–778.
Peixoto, J., Oort, A., 1992. Physics of Climate. American Institute of Physics. 520 pp.
Percival, D.B., Overland, J.E., Mofjeld, H.O., 2001. Interpretation of North Pacific variability as a short- and long-memory process. J. Climate 14, 4545–4559.
Peterson, W.T., Schwing, F.B., 2003. A new climate regime in northeast Pacific ecosystems. Geophys. Res. Lett. 30, 1896. doi:10.1029/2003GL017528.
Philander, S.G.H., 1990. El Niño, La Niña and the Southern Oscillation. Academic Press, San Diego, CA.
PICES, 2004. Marine ecosystems of the North Pacific. PICES Special Publication 1. 280 pp.
Pierce, D.W., 2001. Distinguishing coupled ocean–atmosphere interactions from background noise in the North Pacific. Prog. Oceanogr. 49, 331–352.
Pierce, D.W., Barnett, T.P., Latif, M., 2000. Connections between the Pacific Decadal Oscillation and midlatitudes on decadal time scales. J. Climate 13, 1173–1194.
Pope, J.G., Shepherd, J.G., Webb, J., 1994. Successful surf-riding on size spectra: the secret of survival in the sea. Phil. Trans. Royal Soc. Lond. B 343, 41–49.
Qiu, B., 2003. Kuroshio Extension variability and forcing of the Pacific decadal oscillations: responses and potential feedback. J. Phys. Oceanogr. 33, 2465–2482.
Quadrelli, R., Wallace, J.M., 2004. A simplified linear framework for interpreting patterns of Northern Hemisphere wintertime climate variability. J. Climate 17, 3728–3744.
Royer, T.C., 1998. Coastal processes in the northern North Pacific. In: Robinson, A.R., Brink, K.H. (Eds.), The Global Coastal Ocean: Regional Studies and Synthesis. John Wiley and Sons, Inc., New York, pp. 395–414.
Royer, T.C., 2005. Hydrographic responses at a coastal site in the northern Gulf of Alaska to seasonal and interannual forcing. Deep-Sea Res. II 52, 267–288.
Royer, T.C., Grosch, C.E., 2006. Ocean warming and freshening in the northern Gulf of Alaska. J. Geophys. Res. 33, L16605. doi:10.1029/2006GL026767.
Schwing, F.B., Mendelssohn, R., 1997a. Increased coastal upwelling in the California Current System. J. Geophys. Res. 102, 3421–3438.
Schwing, F.B., Mendelssohn, R., 1997b. Long-term variability in the seasonality of EBC systems: an example of increased upwelling from the California Current. In: Durand, M.H., Cury, P., Mendelssohn, R., Roy, C., Bakun, A., Pauly, D. (Eds.), Global Versus Local Changes in Upwelling Systems: Proceedings of the First International CEOS Workshop. ORSTOM, Paris, pp. 79–99.
Schwing, F.B., Murphree, T., deWitt, L., Green, P.M., 2002. The evolution of oceanic and atmospheric anomalies in the northeast Pacific during the El Niño and La Niña events of 1995–2001. Prog.Oceanogr. 54, 459–491.
Schwing, F.B., Jiang, J., Mendelssohn, R., 2003. Coherency of regime shifts between the NAO, NPI, and PDO. Geophys. Res. Lett. 30, 1406. doi:10.1029/2002GL016535.
Schwing, F.B., Bond, N.A., Bograd, S.J., Mitchell, T., Alexander, M.A., Mantua, N., 2006. Delayed coastal upwelling along the U.S. west coast in 2005: a historical perspective. Geophys. Res. Lett. 33, L22S01. doi:10.1029/2006GL026911.
Stommel, H., Yoshida, K., 1972. Kuroshio: Its Physical Aspects. Univ. of Wash. Press, Seattle.
Strub, P.T., Mesias, J.M., Montecino, V., Rutllant, J., Salinas, S., 1998. Coastal ocean circulation off western South America. In: Robinson, A.R., Brink, K.H. (Eds.), The Global Coastal Ocean: Regional Studies and Synthesis. John Wiley and Sons, Inc., New York, pp. 273–314.
Tatebe, H., Yasuda, I., 2005. Interdecadal variations of the coastal Oyashio from the 1970s to the early 1990s. Geophys. Res. Lett. 32, L10613. doi:10.1029/2005GL022605.
Thompson, D.W.J., Wallace, J.M., 1998. The Arctic Oscillation signature in the wintertime geopotential height and temperature fields. Geophys. Res. Lett. 25, 1297–1300.
Tomita, T., Wang, B., Yasunari, T., Nakamura, H., 2001. Global pattern of decadal-scale variability observed in sea surface temperature and lower-tropospheric circulation fields. J. Geophys. Res. 106, 26805–26815.
Tomita, T., Xie, S.-P., Nonaka, M., 2002. Estimates of surface and subsurface forcing for decadal sea surface temperature variability in the mid-latitude North Pacific. J. Meteor. Soc. Jpn. 80, 1289–1300.
Trenberth, K.E., Hurrell, J.W., 1994. Decadal atmosphere–ocean variations in the Pacific. Clim. Dyn. 9, 303–319.
Walker, G.T., 1924. Correlations in seasonal variations of weather IX. Mem. Ind. Meteorol. Dept. 24, 275–332.
Wallace, J.M., Gutzler, D.S., 1981. Teleconnections in the geopotential height field during the Northern Hemisphere winter. Mon. Weather Rev. 109, 784–812.
Wang, C., Xie, S.-P., Carton, J.A. (Eds.), 2004. Earth's Climate: the ocean–atmosphere interaction. Geophysical Monograph, vol. 147. American Geophysical Union, Washington, DC.
White, W.B., Allan, R.J., 2001. A global quasi-biennial wave in surface temperature and pressure and its decadal modulation from 1900 to 1994. J. Geophys. Res. 106, 26789–26803.